

Article

Physicochemical and Microstructural Characteristics of Sulfated Polysaccharide from Marine Microalga

Diana Fimbres-Olivarria ^{1,*}, Jorge Marquez-Escalante ^{2,*}, Karla G. Martínez-Robinson ²,
Valeria Miranda-Arizmendi ², Yubia De Anda-Flores ², Agustín Rascon-Chu ², Francisco Brown-Bojorquez ³
and Elizabeth Carvajal-Millan ^{2,*}

¹ Department of Scientific and Technological Investigations (DICTUS), University of Sonora, Blvd. Luis Donaldo Colosio, S/N, Hermosillo 83000, Sonora, Mexico

² Research Center for Food and Development (CIAD, AC), Carretera Gustavo Enrique Astiazaran Rosas No. 46, Col. La Victoria, Hermosillo 83304, Sonora, Mexico; karlagm@ciad.mx (K.G.M.-R.); vmiranda222@estudiantes.ciad.mx (V.M.-A.); yubia.deanda@ciad.mx (Y.D.A.-F.); arascon@ciad.mx (A.R.-C.)

³ Department of Polymers, University of Sonora, Blvd. Luis Donaldo Colosio, S/N, Hermosillo 83000, Sonora, Mexico; francisco.brown@unison.mx

* Correspondence: diana.fimbres@unison.mx (D.F.-O.); marquez1jorge@gmail.com (J.M.-E.); ecarvajal@ciad.mx (E.C.-M.); Tel.: +52-662-259-2144 (D.F.-O.); +52-662-289-2400 (E.C.-M.)

Abstract: Marine algae are a valuable source of polysaccharides. However, the information available on sulfated polysaccharides from microalgae is limited. *Navicula* sp. is a microalga present in the Sea of Cortez, of which little is known regarding their polysaccharides' properties. This study investigated the physicochemical and microstructural characteristics of *Navicula* sp. sulfated polysaccharide (NSP). The Fourier transform infrared spectrum of NSP showed distinctive bands (1225 and 820 cm⁻¹, assigned to S–O and C–O–S stretching, respectively), confirming the molecular identity. NSP registered molecular weight, intrinsic viscosity, a radius of gyration, and a hydrodynamic radius of 1650 kDa, 197 mL/g, 61 nm, and 36 nm, respectively. The zeta potential, electrophoretic mobility, conductivity, and diffusion coefficient of the molecule were –5.8 mV, –0.45 μm cm/s V, 0.70 mS/cm, and 2.9 × 10⁻⁹ cm²/s, respectively. The characteristic ratio and persistence length calculated for NSP were 4.2 and 1.3 nm, suggesting a nonstiff polysaccharide chain conformation. The Mark–Houwink–Sakurada α and K constants were 0.5 and 1.67 × 10⁻¹, respectively, indicating a molecular random coil structure. NSP scanning electron microscopy revealed a rough and porous surface. Knowing these polysaccharides' physicochemical and microstructural characteristics can be the starting point for elucidating their structure–function relationship as a valuable tool in advanced biomaterial design.

Keywords: marine diatoms; sulfated polysaccharides; macromolecular characteristics; chain conformation; multi-angle light scattering; scanning electron microscopy; structure–function relationship



Citation: Fimbres-Olivarria, D.; Marquez-Escalante, J.; Martínez-Robinson, K.G.; Miranda-Arizmendi, V.; Anda-Flores, Y.D.; Rascon-Chu, A.; Brown-Bojorquez, F.; Carvajal-Millan, E. Physicochemical and Microstructural Characteristics of Sulfated Polysaccharide from Marine Microalga. *Analytica* **2023**, *4*, 527–537. <https://doi.org/10.3390/analytica4040036>

Academic Editor: Marcello Locatelli

Received: 19 October 2023

Revised: 21 November 2023

Accepted: 29 November 2023

Published: 5 December 2023



Copyright: © 2023 by the authors. Licensee MDPI, Basel, Switzerland. This article is an open access article distributed under the terms and conditions of the Creative Commons Attribution (CC BY) license (<https://creativecommons.org/licenses/by/4.0/>).

1. Introduction

Seaweeds are considered a valuable source of polysaccharides with important bioactive properties since they benefit human health as antiproliferative, antioxidant, and antiviral agents, among other properties [1]. Several studies on obtaining and using polysaccharides from seaweeds mention the potential of the sulfated polysaccharides present in them [2,3]. The structure of polysaccharides depends on their composition and the glycosidic linkage, which determines the conformational flexibility. In addition, whether they are homopolysaccharides or heteropolysaccharides, the molecular weight, the functional groups that the chain presents, and the presence of other covalently linked molecules, such as proteins, influence the macromolecule's characteristics [4]. According to the reported investigations, the polysaccharide's numerous bioactive properties may be due to its molecular weight, sulfate group presence, or negative charge.

Interest in marine microalgae sulfated polysaccharides is growing due to their advantages because they are easy to grow, and the harvest does not depend on any climate or season. Multiple microalgae species release polysaccharides and exopolysaccharides and have been reported to have activity as antiviral agents, antioxidants, anti-inflammatory agents, immunoregulatory agents, and biomedical lubricants [2]. Even though diatoms have proven to be an essential source of diverse compounds, microalgae's sulfated polysaccharide structure has yet to be studied nearly as much as macroalgae. Due to the challenges encountered in collecting clean samples and the complexity of their chemical structure, only a tiny number of microalgae polysaccharide structures have been solved. It is essential to understand the structural and physicochemical characteristics of extracellular polysaccharides to comprehend better their functions and possible applications, which are crucial to their behavior and comprise rheological characteristics and molecular weight [3].

Studying the diverse and varied structural sulfated exopolysaccharides produced by different microalgae is difficult. However, microalgae have the benefit of growing under controlled conditions, which can increase the stability of their polysaccharides' chemical makeup, structural makeup, and rheological behavior, regardless of the length of the collection period [4]. Despite this, the information available on sulfated polysaccharides from marine microalgae is limited. In these organisms, polysaccharides perform several functions, including forming mucilage envelopes and coatings that create a microenvironment around cells that protect them from sudden and adverse environmental changes. Carboxyl and sulfate groups in these polysaccharides ensure detoxification caused by heavy metals [5]. It has been reported that, under stress conditions, an increase in the content of uronic acids, sulfates, and fucose occurs in these polysaccharides to help the microalgae adapt to sudden changes in their environment [6]. Since the characteristics of sulfated polysaccharides from marine microalgae can vary depending on the growth conditions [4], different maritime regions may lead to differences in the structure and functionality of these biopolymers.

Sulfated polysaccharides from several microalgae have been associated with numerous bioactivities that benefit human health, making them compounds of interest and potential applications for the pharmaceutical industry and regenerative medicine. In addition, it has been reported that these polysaccharides did not present cytotoxicity, and they can keep low glycemic levels and exert antioxidant activity simultaneously [7]. Microalgae sulfated polysaccharides have also gained attention for biomedical applications, such as developing tissue engineering scaffolds [8]. Microalgae sulfated polysaccharides have also been considered promising candidates in other sectors, such as the food industry and agriculture [9]. However, more information about these polysaccharides' physicochemical features and morphological characteristics must be generated. Investigating factors such as molecule conformation and surface charge in solution could represent the key to understanding their structure–function relationships.

The present study aimed to investigate the physicochemical and microstructural characteristics of *Navicula* sp. sulfated polysaccharides. *Navicula* sp. is a microalga growing in the Sea of Cortez, of which little is known regarding their polysaccharides. The current investigation combines different techniques to deepen the analysis of these macromolecules as a starting point for understanding their structure–function relationships as a basis for future microalga-sulfated polysaccharide applications.

2. Materials and Methods

Microalga was cultured on a laboratory scale under controlled conditions using white light. The biomass of filtered cells was lyophilized at $-37\text{ }^{\circ}\text{C}/0.133\text{ mbar}$ overnight (Freezone 6 freeze drier Labconco, Kansas, MO, USA) and used to obtain sulfated polysaccharides from microalgae *Navicula* sp. (NSP) as previously reported [4]. Briefly, lyophilized biomass was dispersed in distilled water (1 h, $30\text{ }^{\circ}\text{C}$) and then centrifuged (15 min, $20,000\times g$). The supernatant was precipitated in 65% (*v/v*) ethanol (12 h, $4\text{ }^{\circ}\text{C}$). The precipitate was dried by solvent exchange (80% (*v/v*) ethanol, absolute ethanol, and acetone) to

give NSP. The recovered NSP presented 0.33% sulfate content (weight of sulfate/biomass dry weight) and galactose and glucose as the main carbohydrate components [4]. All chemical reagents were purchased from Sigma-Aldrich Chemical Company (St. Louis, MO, USA).

2.1. Size-Exclusion Chromatography with Multi-Angle Light Scattering

Weight-average molar mass (M_w), number-average molar mass (M_n), intrinsic viscosity ($[\eta]$), the radius of gyration (RG), hydrodynamic radius (R_h), and polydispersity index ($I = M_w/M_n$) were determined using a size-exclusion chromatography (SEC) system on a DAWN HELOS-II 8 multi-angle laser light scattering (MALS) instrument detector coupled with a ViscoStar-II Viscometer and a refractive index (RI) Optilab T-rex detector (Wyatt Technology Corp., Santa Barbara, CA, USA). Samples were dissolved in 50 mM $\text{NaNO}_3/0.02\% \text{NaN}_3$ at 5 mg/mL and 80 °C for one h, then centrifuged (15,000 rpm, 10 min) and filtered (0.45 μm , Millipore, Burlington, MA, USA). A flow rate of 0.7 mL/min in an Agilent HPLC System was used (G1310B Iso-Pump, G1329B autosampler, and G1314F Variable Wavelength Detector, Agilent Technologies, Inc., Santa Clara, CA, USA). The sample was injected into two columns: Shodex OH-pak SBH-Q-804 and 805 (Shodex Showa Denco K.K., Tokyo, Japan). The ASTRA 6.1 software was used. The specific refractive index increment (dn/dc) value of 0.146 mL/g was used [7]. The characteristic ratio (C_∞) and persistence length (q) were calculated according to the following equations [10]:

$$q = (C_\infty + 1) \times I_0/2 \quad (1)$$

and

$$C_\infty = 6 \cdot RG^2 \times M_0/I_0^2 \times M_w \quad (2)$$

In the present study, $I_0 = 0.5 \text{ nm}$ (length of the primary monosaccharide residue), $M_0 = 180 \text{ g/mol}$ (molar mass of the primary monosaccharide residue) [11], and M_w is the molar mass of NSP.

2.2. Dynamic Light Scattering (DLS) Analysis and Phase Analysis Light Scattering (PALS)

Zeta potential (ζ) was determined via dynamic light scattering (DLS), and electrophoretic mobility (μ) was calculated via phase analysis light scattering (PALS) in NSP by using a Möbiu ζ (Wyatt Technology Corp., Santa Barbara, CA, USA) at 25 °C and the software DYNAMICS 7.3.1.15 (Wyatt Technology Corp., Santa Barbara, CA, USA) [10]. The diffusion coefficient and conductivity were also determined from DLS analysis. Distilled water was used as a solvent, and NSP was dispersed at 0.1% (w/v). NSP electrophoretic mobility was calculated by using the following Smoluchowski equation [12]:

$$\mu = \varepsilon \zeta / \eta \quad (3)$$

where μ is the electrophoretic mobility, ζ is the zeta potential, ε is the electric permittivity of the liquid (79), and η is the viscosity (0.89 cP).

2.3. Fourier Transform Infrared (FTIR) Spectroscopy

FTIR spectrum of dry NSP powder was recorded on a Nicolet iS50 FT-RI Spectrometer (Madison, WI, USA). The sample was examined by iS50 ATR analysis. Spectrum was recorded in the 4000 to 400 cm^{-1} [4].

2.4. Scanning Electron Microscopy

The sample was frozen at $-20 \text{ }^\circ\text{C}$ and lyophilized ($-37 \text{ }^\circ\text{C}/0.133 \text{ mbar}$ overnight) in a Freezone 6 freeze drier (Labconco, Kansas, MO, USA). NSP was analyzed by field emission scanning electron microscopy (SEM) (JEOL 5410LV, JEOL, Peabody, MA, USA) using a voltage of 10 kV and $100\times$ or $5000\times$ magnifications. SEM images were obtained in secondary and backscattered electron imaging modes [7].

3. Results

3.1. Size-Exclusion Chromatography with Multi-Angle Light Scattering

Polysaccharides are polydisperse; they might present different conformations and molecular weights, among other molecule characteristic variations. In this regard, combining size-exclusion chromatography with multi-angle light scattering (SEC-MALS) represents an advanced technique for the absolute characterization of these macromolecules [7]. The SEC column separates the molecules by hydrodynamic volume, passing them through an MALS detector. In addition to MALS signals, UV absorbance and differential refractive index (dRI) detectors characterize the molecule's physical properties. Furthermore, a differential viscometer can determine the intrinsic viscosity value for polymers such as polysaccharides. The present study investigated NSP macromolecular characteristics such as molar mass, size, and conformation using SEC-MALS, as these are basic physical properties for polymer characterization. Fundamental knowledge generated by SEC-MALS might be worthwhile for advanced NSP characterization and application.

The elution profile of NSP is presented in Figure 1, where dRI, UV, light scattering (LS), and degree of polymerization (DP) are shown. NSP registered quadrimodal LS response with the prominent peak eluting before the central dRI peak. This NSP elution profile indicates polydispersity, as confirmed by the DP signal. UV peaks at high elution times in NSP could be related to low molar mass residual proteins [13].

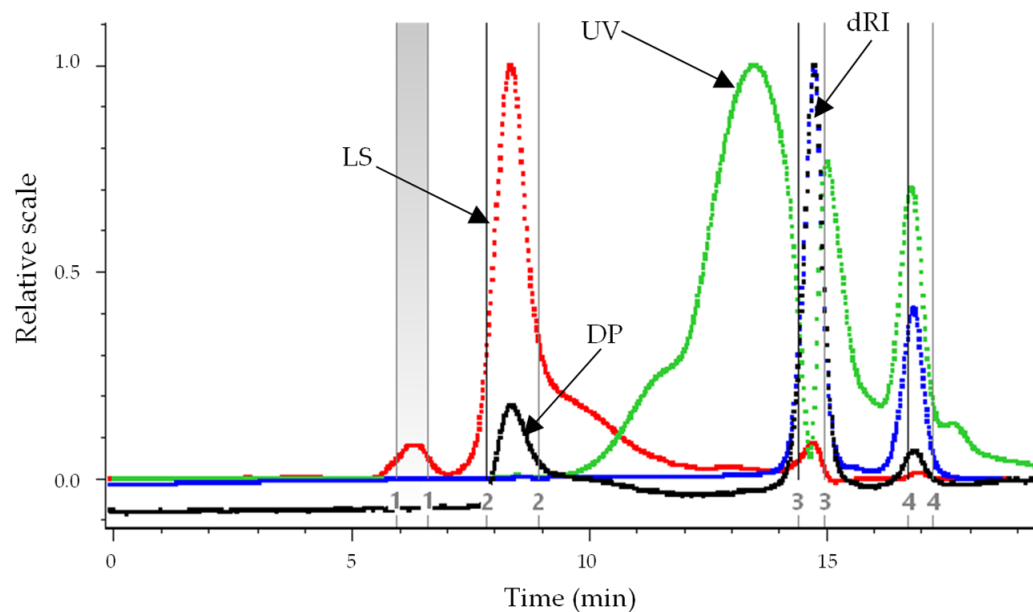


Figure 1. Size-exclusion chromatography with multi-angle light scattering (SEC-MALS) of sulfated polysaccharide from microalgae *Navicula* sp. (NSP). Differential refractive index dRI (blue line), light scattering LS (red line), ultraviolet UV (green line), and degree of polymerization DP (black line). LS population number 1, 2, 3, and 4 are indicated.

The macromolecular characteristics of NSP are presented in Table 1. NSP's molecular weight (Mw) value was 1650 kDa, within the range reported for other sulfated polysaccharides from microalga. Sulfated polysaccharides have been reported to register an Mw of 45 kDa in *Navicula inserta* and 4810 kDa in *Phaeodactylum tricorutum* [14,15]. The polydispersity index (PI), intrinsic viscosity $[\eta]$, radius of gyration (RG), hydrodynamic radius (Rh), and α and K Mark–Houwink–Sakurada values registered for NSP are close to those reported in the literature for these macromolecules in another microalga [7,16]. The NSP α exponent registered was within the limits (0.5–0.8) reported in the literature for a flexible coil conformation in polymer chains [17]. In the present study, characteristic ratio (C_∞) and persistence length (q) parameters are reported for the first time for sulfated polysac-

charides from microalgae. q values for NSP were lower than those reported for macroalga polysaccharides such as alginate [18].

Table 1. Macromolecular characteristics of sulfated polysaccharide from microalgae *Navicula* sp. (NSP) determined by size-exclusion chromatography with multi-angle light scattering (SEC-MALS).

| | |
|--------------------------------|-----------------------|
| Mw (kDa) | 1650 |
| PI (Mw/Mn) | 1.34 |
| $[\eta]$ (mL/g) | 197 |
| RG (nm) | 61 |
| Rh (nm) | 36 |
| C_∞ | 4.2 |
| q (nm) | 1.3 |
| Mark–Houwink–Sakurada α | 0.5 |
| Mark–Houwink–Sakurada K (mL/g) | 1.67×10^{-1} |

Mw: weight-average molar mass; Mn: number-average molar mass; PI: polydispersity index; $[\eta]$: intrinsic viscosity; RG: radius of gyration; Rh: hydrodynamic radius; C_∞ : characteristic ratio; q : persistence length.

3.2. Physical Properties

Dynamic light scattering (DLS) allows for determining the particle size of suspended material that is freely moving (Brownian motion). The sample is exposed to alternating positive and negative currents (electrophoresis), and the particle movement towards either the positive or negative pole is monitored. The direction of the motion relates to the sign (positive/negative) of the zeta potential, and the movement's rate relates to the zeta potential's magnitude [12]. A schematic representation of zeta potential is presented in Figure 2. The liquid layer surrounding the macromolecule has two parts: an inner region (Stern layer) where the ions are firmly bound and an outer (diffuse) region where they are less firmly associated. The diffuse layer has a boundary with which the ions and the molecule form a stable structure. When a particle moves, the ions beyond the boundary stay with the bulk. The potential at this boundary is the zeta potential (ζ).

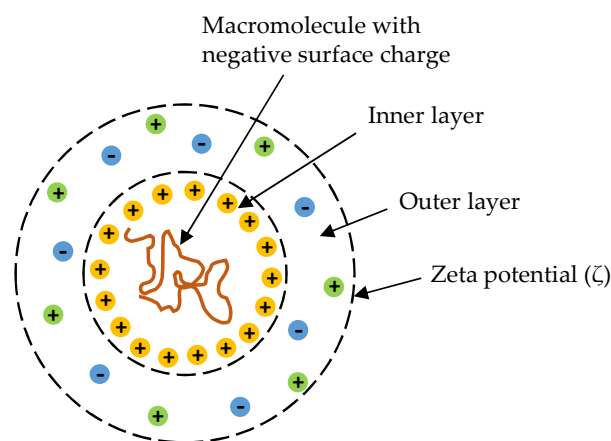


Figure 2. Schematic representation of zeta potential (ζ).

NSP physical properties (ζ potential, electrophoretic mobility, conductivity, and diffusion coefficient) are reported in Table 2. The ζ potential is a parameter that measures the electrochemical equilibrium at the particle–liquid interface of suspended macromolecules or particles. It can be used to optimize biopolymer formulations, predict surface interactions, and predict long-term stability, among others. The ζ potential represents the charge at the interface between a solid surface and its liquid medium. In the present study, NSP registered a ζ potential value of -5.7 mV. As an anionic polysaccharide, NSP was expected to be negatively charged at pH 6.0 due to the sulfate content. This low ζ potential indicates that the electrostatic repulsion between molecules is weak, which decreases the system's stability, resulting in the formation of NSP aggregates. The self-assembly of polysaccharide

solutions is favored by the hydrophobic interactions between the molecules, resulting in aggregate formation. Nevertheless, this behavior is defined by the polysaccharide chemical structure and charge, resulting in different ζ potential ranges [19]. When an electric field is applied across an electrolyte, charged particles suspended are attracted toward the electrode of the opposite charge. The velocity of a particle in an electric field is referred to as its electrophoretic mobility (μ). It is known that μ is directly proportional to the zeta potential while it will vary inversely with conductivity (Henry Equation). The ζ potential can also indicate the variation in the observed mobility [12]. In addition, DLS measures fluctuations in scattered light intensity due to diffusing particles, and the diffusion coefficient of the particles can be determined. In the present study, the electrophoretic mobility (μ), conductivity, and diffusion coefficient (D) of NSP were lower than those reported for carrageenan [20], which could be due to a small sulfate content in NSP concerning carrageenan. These physicochemical properties could help interpret and predict NSP molecular behavior under aqueous conditions.

Table 2. Zeta potential, mobility, diffusion, and conductivity values of sulfated polysaccharide from microalgae *Navicula* sp. (NSP) determined by dynamic light scattering (DLS) analysis and phase analysis light scattering (PALS).

| | |
|---|--|
| Zeta potential (ζ) (mV) | -5.80 ± 0.13 |
| Electrophoretic mobility (μ) ($\mu\text{m cm/s V}$) | -0.45 ± 0.01 |
| Conductivity (mS/cm) | 0.70 ± 0.01 |
| Diffusion coefficient (D) (cm^2/s) | $2.90 \times 10^{-9} \pm 1.90 \times 10^{-10}$ |

Measurements at 25 °C. Water as solvent. Results are expressed as mean \pm SD.

3.3. Fourier Transform Infrared (FTIR) Spectroscopy

FTIR is a rapid and nondestructive analytical technique extensively used for structural characterization of molecules. It is based on the interference of light. A computer transforms the measured interferogram into an infrared spectrum through Fourier transforms. This technique is widely used for molecular structure elucidation. However, spectrum interpretation and band assignment can be difficult for complex macromolecules such as polysaccharides. The FTIR spectrum of NSP is presented in Figure 3. Characteristic peaks described in the literature are indicated in this FTIR spectrum.

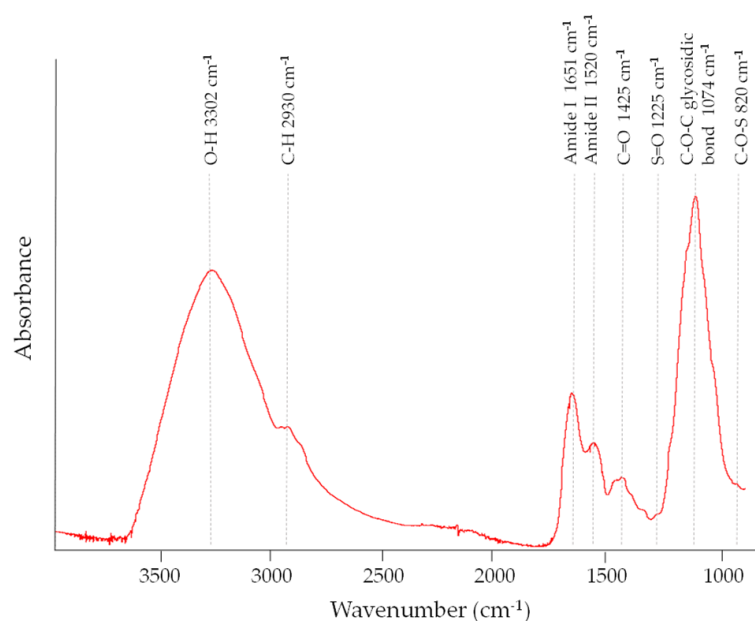


Figure 3. Fourier transform infrared (FT-IR) spectrum of sulfated polysaccharide from *Navicula* sp. (NSP). The dotted lines indicate the assignment of the peaks analyzed.

The bands detected in NSP confirm that the sample corresponds to a sulfated polysaccharide [4,7]. Sulfated polysaccharides present characteristic absorption bands in FTIR spectroscopy ($1200\text{--}1270\text{ cm}^{-1}$ and $900\text{--}800\text{ cm}^{-1}$, corresponding to the stretching of S–O and the stretching of C–O–S, respectively), which are assigned to the sulfate groups in these molecules.

3.4. Scanning Electron Microscopy (SEM)

As shown in Figure 4, SEM images revealed a relatively uniform surface in NSP and a rough and porous morphology. Similar microstructural characteristics have been previously reported in marine polysaccharides from algae [7,21]. SEM is a valuable technique for studying polysaccharide microstructural morphology. The SEM is based on the principle that the magnetic field can deflect electrons. This technique replaces the light source with a high-energy electron beam. The SEM-focused electron beam scans across the sample's surface, generating significant signals, which are then converted to a visual signal [22]. SEM allows visualization of the polysaccharide surfaces at submicron scales. The sample surface must be electrically conductive or be sputtered by powdered conductive materials such as gold.

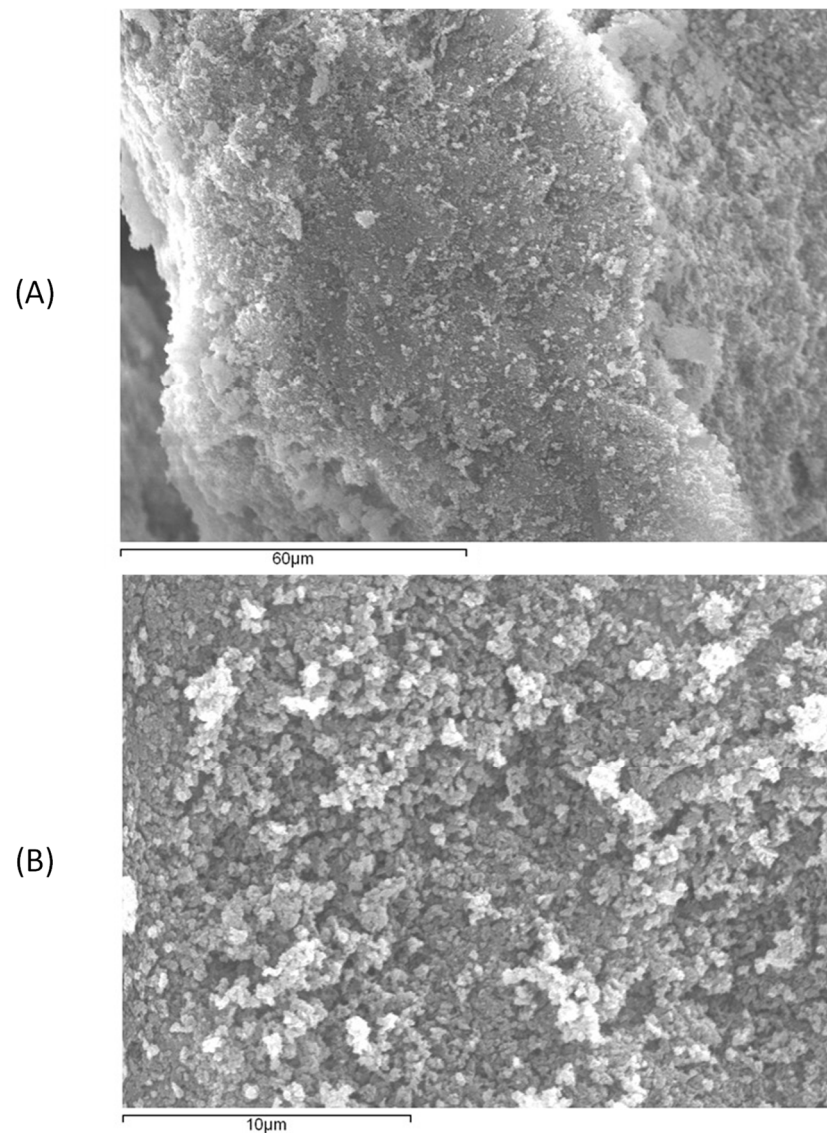


Figure 4. Scanning electron microscopy (SEM) images of lyophilized sulfated polysaccharide extracted from *Navicula* sp. (NSP) at $1000\times$ (A) and $5000\times$ (B) magnifications.

4. Discussion

Mw determination by SEC-MALS is based on light scattering intensity and sample concentration, allowing the detection of aggregates. In this regard, small polysaccharide mass fractions presenting a high Mw close to the value of the other mass fractions in the elution profile may result in a calculated high Mw value for the sample. Moreover, in macromolecules, differences in conformation, aggregation, and polyelectrolyte expansion, among other effects, can affect the molecular separation profile [23,24]. As presented in Figure 1, NSP is a polydisperse macromolecule, a common polysaccharide characteristic. In addition, it is known that the characteristics of sulfated polysaccharides from microalgae depend on the species and the culture conditions [14].

NSP polydispersity index (PI) and intrinsic viscosity $[\eta]$ are close to the values reported for other microalga-sulfated polysaccharides such as *Chatoceros muelleri* [7] (Table 1). As determined by dynamic light scattering, Rh represents the radius of an equivalent hard sphere diffusing at the same rate as the molecule under observation. Dispersed polysaccharides do not exist as hard spheres, but Rh means the apparent size the solvated molecule adopts in motion. RG is the mass-weighted average distance from the molecule center to each mass element in this. For macromolecules with $RG > 10$ nm, this value is determined by measuring a difference in the intensity of scattered light at different angles (angular dependence) [25]. Rh and RG values in sulfated polysaccharides from microalga are scarce in the literature. An Rh value of 1.33 nm was found for sulfated endo polysaccharides from *Chatoceros muelleri* [7]. RG from 148 to 176 nm was found for sulfated exopolysaccharides from *Porphyridium cruentum* [26].

Both C_{∞} and q values calculated in the present study for NSP are small compared to those reported for other polysaccharides such as galactomannan ($9 < C_{\infty} < 16$ and $3 < q < 5$ nm). It has been suggested that polysaccharides may already present more considerable persistence lengths than those calculated, being probably stabilized by intramolecular aggregation [17]. The NSP q value (1.3 nm) was lower than those reported for alginate from macroalga (12–16 nm) [16], suggesting that NSP chains are less stiff than alginate chains and might be considered relatively flexible compared to very rigid macromolecules such as xanthan ($q \sim 120$ nm). An accurate characterization of q in NSP is fundamental, as the chain flexibility can affect the macromolecule inter- and intra-interaction and adhesion with cell surface [17,18]. The Mark–Houwink–Sakurada equation is related to intrinsic viscosity; in this equation, K and α are used to study polysaccharide conformation. The exponent α is related to chain conformation; values of 1.26 and 0.50 correspond to very rigid and random coil structures, respectively. In addition, high K values indicate an expanded coil conformation, while low K values represent a compact coil conformation [10]. NSP presented α and K values that suggest a molecular random coil structure, this study being the first report on these macromolecule conformational characteristics (Table 1).

The charge density on their surface is the main factor affecting the interaction between charged molecules. The ζ potential value is an essential tool to measure the electrical charge of a molecule's surface. It indicates electrostatic repulsion between adjacent, similarly charged particles in dispersion. Therefore, ζ potential can be an indicator of macromolecule dispersion stability. A small ζ potential value suggests that attractive forces may exceed electrostatic repulsion, and the dispersion could flocculate.

Consequently, macromolecules presenting high ζ potential (negative or positive) are electrically stabilized, while those showing low values tend to aggregate and precipitate. It is considered that when the ζ potential value is higher than 30 mV or less than -30 mV, electrostatic repulsions between particles minimize their aggregation [12]. The NSP ζ potential value found in the present study suggests that this polysaccharide could form aggregates under the experimental conditions used (Table 2). NSP registered lower ζ potential, electrophoretic mobility (μ), and diffusion coefficient (D) than those reported for carrageenan (-100 mV, 4.9 cm²/s, and -6.3 μ m cm/s V, respectively), which could be partly attributed to the different sulfate content in these two polysaccharides (0.33%

for NSP and 20% for carrageenan). A decrease in the D value could be related to a more extended polysaccharide conformation.

Regarding μ , which represents the molecule migration velocity under the applied electric field, the negative value confirms that the electrokinetic charge of NSP is negative under the experimental conditions used. About NSP conductivity, this property could be essential for developing ion exchange membranes based on this polymer, which may be helpful in polymer electrolyte fuel cells. From a sustainable point of view, using microalgae as a source of natural polymers containing sulfate groups that enable proton motion is an attractive option for tailoring biobased membranes. These results facilitate the prediction and proper interpretation of NSP as functional macromolecules for applications where physicochemical properties are determinant, such as micro- and nano-biomaterial fabrication or as thickening agents in formulations.

In the FTIR spectrum of NSP (Figure 3), polysaccharide characteristic regions were distinguished as, for example, OH and CH stretching vibrations at 3600–2800 cm^{-1} . The band in the region of 3405 cm^{-1} corresponds to OH groups; a similar band around this wavenumber was observed for sulfated polysaccharides from green and brown seaweeds. A region of local symmetry at 1500–1200 cm^{-1} , a region of CO stretching vibration at 1200–950 cm^{-1} , a fingerprint or anomeric region at 950–700 cm^{-1} , and a skeletal region below 700 cm^{-1} were registered. The small band observed at 1244 cm^{-1} indicates the presence of S=O groups; some studies have reported this band's existence in sulfated polysaccharides extracted from the three major groups of seaweeds (green, brown, and red algae) [27]. This analysis confirms the molecular identity of NSP as a sulfated polysaccharide. In this regard, FTIR spectroscopy can be an excellent tool for the preliminary identification of microalgae polysaccharides.

SEM is a robust analysis that reveals the morphological characteristics of polysaccharides, for example, cavities or porous size and surface or internal regularity. In macromolecule research, the study of the molecule's morphological characteristics and architectures using SEM is a primary tool for creating polymeric natural-based materials inspired by the microstructure. SEM is also essential for featuring biomaterials' morphological characterization and structural defect analysis.

The SEM analysis allowed for achieving spatial and complementary information on the NSP powder, which is fundamental for studying the morphological properties, such as particle size, material porosity, and tridimensional shape [28]. In the current investigation, NSP revealed porous nature surface topography under SEM analysis (Figure 4). Similar SEM observations with a rough appearance have been reported for other sulfated polysaccharides from microalgae [4,7]. Polysaccharide morphology could determine physical characteristics, such as solubility, water absorption capacity, and emulsification capacity.

A better understanding of NSP physicochemical properties and microstructural characteristics is critically essential to generate insights into the structure–function relationship of this macromolecule. In the future, this information might be the key to proposing innovative applications for this polysaccharide, especially in pharmaceutical and biomedical applications. Nevertheless, further research on NSP structure–bioactivity relationships and mechanisms must be performed to explore the molecule's potential application in several areas, such as biomedicine or pharmaceuticals. In addition, it would be interesting to explore chemical or enzymatical modifications of these polysaccharides, looking for specialized functions, as these macromolecules can improve their physical characteristics through structural modifications.

5. Conclusions

Physicochemical properties and microstructural characteristics of *Navicula* sp. sulfated polysaccharide (NSP) were investigated. The molecular identity of NSP was confirmed by Fourier transform infrared spectrometry. The polysaccharide molecular weight, intrinsic viscosity, radius of gyration, and hydrodynamic radius were in the range reported for other sulfated polysaccharides from microalgae. The zeta potential, electrophoretic mobility,

and diffusion coefficient of NSP were smaller than those informed for macroalgae sulfated polysaccharides, which could be attributed to the low sulfate content in the former. The molecule's characteristic ratio and persistence length suggest a flexible random coil chain conformation structure. Scanning electron microscopy revealed a rough and porous surface in NSP. Knowing these polysaccharides' macromolecular and microstructural characteristics can be the starting point for elucidating their structure–function relationship as a valuable tool in advanced biomaterial design. This study contributes to advancing knowledge of microalgae sulfated polysaccharides, especially on *Navicula* sp. growing in the Sea of Cortez, of which little is known regarding their polysaccharides' properties.

Author Contributions: Conceptualization, E.C.-M. and D.F.-O.; methodology, J.M.-E., V.M.-A., K.G.M.-R., Y.D.A.-F., A.R.-C. and F.B.-B.; software, J.M.-E. and K.G.M.-R.; validation, E.C.-M. and D.F.-O.; formal analysis, E.C.-M. and D.F.-O.; investigation, E.C.-M. and D.F.-O.; resources, E.C.-M.; data curation, J.M.-E., V.M.-A., K.G.M.-R., Y.D.A.-F., A.R.-C. and F.B.-B.; writing—original draft preparation, E.C.-M. and D.F.-O.; writing—review and editing, J.M.-E., V.M.-A., K.G.M.-R., Y.D.A.-F., A.R.-C. and F.B.-B.; visualization, E.C.-M. and D.F.-O.; supervision, J.M.-E., V.M.-A., K.G.M.-R., Y.D.A.-F., A.R.-C. and F.B.-B.; project administration, E.C.-M.; funding acquisition, E.C.-M. All authors have read and agreed to the published version of the manuscript.

Funding: This research was funded by CONAHCYT, grant number 319684 to E. Carvajal-Millan.

Data Availability Statement: The data are not publicly available due to patent claims in process.

Acknowledgments: The authors are pleased to acknowledge Campa-Mada Alma for technical assistance.

Conflicts of Interest: The authors declare no conflict of interest.

References

1. Beaumont, M.; Tran, R.; Vera, G.; Niedrist, D.; Rousset, A.; Pierre, R.; Forget, A. Hydrogel-forming algae polysaccharides: From seaweed to biomedical applications. *Biomacromolecules* **2021**, *22*, 1027–1052. [[CrossRef](#)] [[PubMed](#)]
2. Ibrahim, M.I.; Amer, M.S.; Ibrahim, H.A.; Zaghoul, E.H. Considerable production of ulvan from *Ulva lactuca* with special emphasis on its antimicrobial and anti-fouling properties. *Appl. Biochem. Biotechnol.* **2022**, *194*, 3097–3118. [[CrossRef](#)] [[PubMed](#)]
3. Orvain, F.; Galois, R.; Barnard, C.; Sylvestre, A.; Blanchard, G.P.; Sauriau, G. Carbohydrate production in relation to microphytobenthic biofilm development: An integrated approach in a tidal mesocosm. *Microb. Ecol.* **2003**, *45*, 237–251. [[CrossRef](#)] [[PubMed](#)]
4. Fimbres-Olivarria, D.; López-Elías, J.A.; Carvajal-Millán, E.; Márquez-Escalante, J.A.; Martínez-Córdova, L.R.; Miranda-Baeza, A.; Enríquez-Ocaña, F.; Valdéz-Holguín, J.E.; Brown-Bojórquez, F. *Navicula* sp. Sulfated Polysaccharide Gels Induced by Fe(III): Rheology and Microstructure. *Int. J. Mol. Sci.* **2016**, *17*, 1238. [[CrossRef](#)] [[PubMed](#)]
5. Shniukova, E.I.; Zolotareva, E.K. Diatom Exopolysaccharides: A Review. *Int. J. Algae* **2015**, *17*, 50–67. [[CrossRef](#)]
6. Gügi, B.; Le Costaouec, T.; Burel, C.; Lerouge, P.; Helbert, W.; Bardor, M. Diatom-specific oligosaccharide and polysaccharide structures help to unravel biosynthetic capabilities in diatoms. *Mar. Drugs* **2015**, *13*, 5993–6018. [[CrossRef](#)]
7. Miranda-Arizmendi, V.; Fimbres-Olivarria, D.; Miranda-Baeza, A.; Martínez-Robinson, K.; Rascón-Chu, A.; De Anda-Flores, Y.; Lizardi-Mendoza, J.; Mendez-Encinas, M.A.; Brown-Bojórquez, F.; Canett-Romero, R.; et al. Sulfated Polysaccharides from *Chaetoceros muelleri*: Macromolecular Characteristics and Bioactive Properties. *Biology* **2022**, *11*, 1476. [[CrossRef](#)]
8. Halperin-Sternfeld, M.; Netanel Liberman, G.; Kannan, R.; Netti, F.; Ma, P.X.; Arad, S.M.; Adler-Abramovich, L. Thixotropic Red Microalgae Sulfated Polysaccharide-Peptide Composite Hydrogels as Scaffolds for Tissue Engineering. *Biomedicines* **2022**, *10*, 1388. [[CrossRef](#)]
9. Moreira, J.B.; Vaz, B.D.S.; Cardias, B.B.; Cruz, C.G.; Almeida, A.C.A.D.; Costa, J.A.V.; Morais, M.G.D. Microalgae Polysaccharides: An Alternative Source for Food Production and Sustainable Agriculture. *Polysaccharides* **2022**, *3*, 441–457. [[CrossRef](#)]
10. De Anda-Flores, Y.; Carvajal-Millan, E.; Lizardi-Mendoza, J.; Rascon-Chu, A.; Tanori-Cordova, J.; Martínez-López, A.L.; Burgara-Estrella, A.J.; Pedroza-Montero, M.R. Conformational Behavior, Topographical Features, and Antioxidant Activity of Partly De-Esterified Arabinoxylans. *Polymers* **2021**, *13*, 2794. [[CrossRef](#)]
11. Vincken, J.P.; Schols, H.A.; Oomen, R.J.; McCann, M.C.; Ulvskov, P.; Voragen, A.G.; Visser, R.G. If homogalacturonan were a side chain of rhamnogalacturonan I. Implications for cell wall architecture. *Plant Physiol.* **2003**, *132*, 1781–1789. [[CrossRef](#)] [[PubMed](#)]
12. Hunter, R.J. *Zeta Potential in Colloid Science*; Academic Press: New York, NY, USA, 1981.
13. Goh, K.K.T.; Pinder, D.N.; Hall, C.E.; Hemar, Y. Rheological and light scattering properties of flaxseed polysaccharide aqueous solutions. *Biomacromolecules* **2006**, *7*, 3098–3103. [[CrossRef](#)] [[PubMed](#)]
14. González-Vega, R.I.; Del-Toro-Sánchez, C.L.; Moreno-Corral, R.A.; López-Elías, J.A.; Reyes-Díaz, A.; García-Lagunas, N.; Carvajal-Millán, E.; Fimbres-Olivarria, D. Sulfated Polysaccharide-Rich Extract from *Navicula Incerta*: Physicochemical Characteristics, Antioxidant Activity, and Anti-Hemolytic Property. *AIMS Bioeng.* **2022**, *9*, 364–382. [[CrossRef](#)]

15. Yang, S.; Wan, H.; Wang, R.; Hao, D. Sulfated Polysaccharides from *Phaeodactylum Tricornutum*: Isolation, Structural Characteristics, and Inhibiting HepG2 Growth Activity In Vitro. *PeerJ* **2019**, *7*, e6409. [[CrossRef](#)] [[PubMed](#)]
16. Miranda-Arizmendi, V.; Carvajal-Millan, E.; Fimbres-Olivarria, D.; Miranda-Baeza, A.; Martínez-Robinson, K.; De Anda-Flores, Y.; Lizardi-Mendoza, J.; Rascón-Chu, A. Macromolecular Characteristics of Sulfated Extracellular Polysaccharides from *Chaetoceros muelleri*. In Proceedings of the 2nd International Electronic Conference on Diversity (IECD 2022)—New Insights into the Biodiversity of Plants, Animals and Microbes, Online, 15–31 March 2022.
17. Picout, D.R.; Ross-Murphy, S.B.; Errington, N.; Harding, S.E. Pressure cell assisted solubilization of xyloglucans: Tamarind seed polysaccharide and detarium gum. *Biomacromolecules* **2003**, *4*, 799–807. [[CrossRef](#)] [[PubMed](#)]
18. Maciel, B.; Oelschlaeger, C.; Willenbacher, N. Chain flexibility and dynamics of alginate solutions in different solvents. *Colloid. Polym. Sci.* **2020**, *298*, 791–801. [[CrossRef](#)]
19. Tüzüm, D.; Ergün, A.P. Assessment of the effect on the plasticizer diffusion of inorganic fillers in plasticized poly(vinyl chloride) composite films for cable sheath applications. *J. Appl. Polym. Sci.* **2023**, *140*, e53996. [[CrossRef](#)]
20. Carneiro-da-Cunha, M.G.; Cerqueira, M.A.; Souza, B.W.S.; Teixeira, J.A.; Vicente, A.A. Influence of concentration, ionic strength and pH on zeta potential and mean hydrodynamic diameter of edible polysaccharide solutions envisaged for multilayered films production. *Carbohydr. Polym.* **2011**, *85*, 522–528. [[CrossRef](#)]
21. De Jesus Raposo, M.F.; De Moraes, A.M.B.; De Moraes, R.M.S.C. Marine polysaccharides from algae with potential biomedical applications. *Mar. Drugs* **2015**, *13*, 2967–3028. [[CrossRef](#)]
22. Zhou, W.; Apkarian, R.; Wang, Z.L.; Joy, D. Fundamentals of Scanning Electron Microscopy (SEM). In *Scanning Microscopy for Nanotechnology*; Zhou, W., Wang, Z.L., Eds.; Springer: New York, NY, USA, 2006. [[CrossRef](#)]
23. Some, D.; Razinkov, V. High-throughput analytical light scattering for protein quality control and characterization. In *High-Throughput Protein Production and Purification*; Vincentelli, R., Ed.; Springer: New York, NY, USA, 2019; pp. 335–359.
24. Boymirzaev, A.S.; Turaev, A.S. Non-exclusion effects in aqueous size exclusion chromatography of polysaccharides. *Chin. Med.* **2010**, *1*, 28–29. [[CrossRef](#)]
25. Tarazona, P.; Saiz, E. Combination of SEC/MALS experimental procedures and theoretical analysis for studying the solution properties of macromolecules. *J. Biochem. Biophys. Methods* **2003**, *56*, 95–116. [[CrossRef](#)] [[PubMed](#)]
26. Balti, R.; Le Balc'h, R.; Brodu, N.; Gilbert, M.; Le Gouic, B.; Le Gall, S.; Siquin, C.; Massé, A. Concentration and purification of *Porphyridium cruentum* exopolysaccharides by membrane filtration at various cross-flow velocities. *Process Biochem.* **2018**, *74*, 175–184. [[CrossRef](#)]
27. Hong, T.; Yin, J.-Y.; Nie, S.-P.; Xie, M.-Y. Applications of infrared spectroscopy in polysaccharide structural analysis: Progress, challenge and perspective. *Food Chem. X* **2021**, *12*, 100168. [[CrossRef](#)] [[PubMed](#)]
28. Wang, Y.; Dykes, G.A. Surface Properties of Polysaccharides. In *Polysaccharides*; Ramawat, K., Mérillon, J.M., Eds.; Springer: Cham, Switzerland, 2014. [[CrossRef](#)]

Disclaimer/Publisher's Note: The statements, opinions and data contained in all publications are solely those of the individual author(s) and contributor(s) and not of MDPI and/or the editor(s). MDPI and/or the editor(s) disclaim responsibility for any injury to people or property resulting from any ideas, methods, instructions or products referred to in the content.